Geological Quarterly, 2004, **48** (4): 371–382

The Zadnie Kamienne "ravenous" shear zone (High-Tatric Nappe) — conditions of deformation

Edyta JUREWICZ and Ewa SŁABY

Jurewicz E. and Słaby E. (2004) — The Zadnie Kamienne "ravenous" shear zone (High-Tatric Nappe) — conditions of deformation. Geol. Quart., **48** (4): 371–382. Warszawa.

The Zadnie Kamienne shear zone is a high-angle Riedel type shear zone (R'), exhibiting an antithetic sense of displacement, which may have developed synchronously with the nappe-thrusting of the Giewont Unit (High-Tatric Nappe). The amount of displacement along this zone is very low and does not explain the very intense deformation, which is of the same character as that at the base of the Giewont Unit (mylonitization, stylolitization and vein forming). The explanation of this phenomenon lies in the multiple activity of this zone, the change of the direction of movement and the important role of pressure solution in hydrothermal conditions responsible for dissolution creep, mass loss and stress relaxation. This kind of shear can be referred to as a "ravenous" shear zone. Neo-forming minerals accompanying these processes were applied as a temperature gauge. Simultaneous growth of albite and adularia indicates a temperature of about 350°C. Chlorites accompanying them occur in two thermal episodes, the first of which indicating a similar temperature (292–357°C).

Edyta Jurewicz and Ewa Słaby, Faculty of Geology, Warsaw University, Żwirki i Wigury 93, PL-02-089 Warsaw, Poland; e-mails: edytaj@geo.uw.edu.pl, E.Slaby@uw.edu.pl *(received: December 12, 2003; accepted: June 24, 2004).*

Key words: Tatra Mts., Carpathians, shear zone, pressure solution, feldspar growth, geothermometers.

INTRODUCTION

The Tatra Mountains (Inner Carpathians) are composed of a crystalline core, overlain by a High-Tatric Mesozoic sedimentary cover and two nappes, the High-Tatric (Tatrikum) and Krížna Nappes (Fig. 1A). In the Tatra Mts., Alpine-style thrusting and folding are of post-Turonian age and linked with the Mediterranean phase (Andrusov, 1965). Analysis of the geometry of the Alpine thrusts and faults in the Tatra Mts. is difficult due to the ductile character of deformation accompanied by a high activity of pressure solution processes (Bac-Moszaszwili *et al*., 1981; Jaroszewski, 1982). The unique character of the surface studied lies in the fact that it cuts both crystalline (in its upper part) as well as various sedimentary rocks, allowing analysis of the influence of rheological properties of rocks on the deformation character within one dislocation zone, that is, within the same conditions. An equally important issue concerns the minor amount of displacement and inadequate strength of deformation.

This paper presents the character, rheological behaviour and temperatures of the deformation processes obtained from the semi-vertical shear zone of Zadnie Kamienne (Fig. 1B, C) cutting the different lithological units of the Giewont and Czerwone Wierchy Units (High-Tatric Nappe).

GEOLOGICAL SETTING

Several structural elements belonging to the High-Tatric Nappe occur in the Czerwone Wierchy Massif on the northern slopes of Ciemniak Mt. (Fig. 1B, C). The highest is represented by the Giewont Unit, comprising crystalline rocks — granites and gneisses, as well as blue-black limestones of Triassic age (Kotański, 1959), building the peak of Chuda Turnia Mt. The lower structural unit is represented by the Czerwone Wierchy Nappe, divided into two elements — the Zdziary and Organy units, which is thrusted on to the autochthonous High-Tatric sedimentary cover (Kominy Tylkowe series). From the top, the Giewont Unit is sheared by the Gładkie Upłaziańskie Slice included within the Križna Nappe (Kotański, 1965). Tectonic interpretations of this area were discussed by Krajewski (1980) and Bac-Moszaszwili *et al*. (1984). Kotański (1959) worked out the lithostratigraphic column of the Zadnie Kamienne area, with almost 40 lithological units.

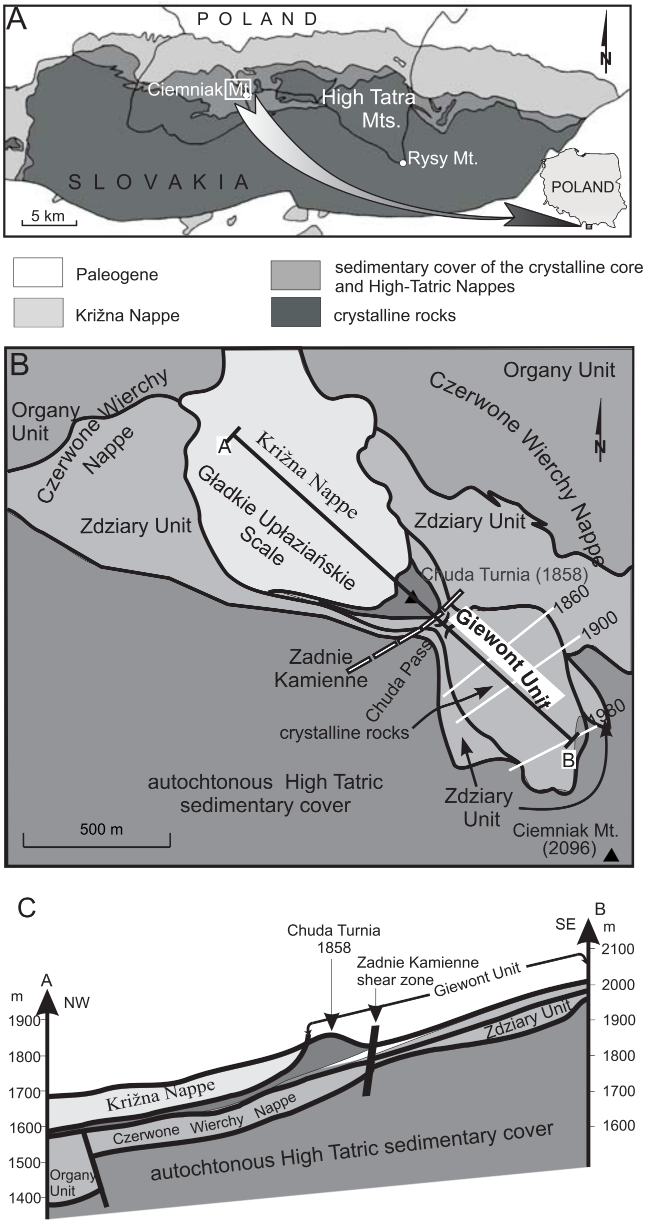

Fig. 1. A — study area in relation to the main geological tectonic structures of the Tatra Mts. (after Bac-Moszaszwili *et al*., 1979); B — tectonic sketch of the vicinity of the study area near Ciemniak Mt. (after Guzik, 1959); white lines — structural isohypses at the base of the Giewont Unit; C — schematic cross-section through the northern slope of Ciemniak Mt., Czerwone Wierchy Nappe

METHODOLOGY

The results of direct field observations and structural analysis are given in the first part (Fig. 2). Observations of structures and textures were carried out on polished surfaces (Fig. 3) and thin sections analysed using a binocular (Fig. 4), an optical microscope (Fig. 5) and microprobe (BSE images — Fig. 6). The minerals were recognised using an optical microscope, and the chemical composition was determined by microprobe analysis (Tables 1–3). In order to determine the temperature conditions of the deformation and hydrothermal processes linked with them, feldspar (Nekvasil and Burnham, 1987; Fuhrmann and Lindsley, 1988) and chlorite geothermometers (Cathelineau, 1988) were applied.

FIELD OBSERVATIONS AND GEOMETRICAL ANALYSIS

The Zadnie Kamienne is a couloir running downwards from the Chuda Pass along a ~ 60/80N oriented tectonic shear zone (Fig. 1B, C). This zone cuts the above-mentioned lithostratigraphic units from the crystalline rocks of the Giewont Unit core to the contact of the Czerwone Wierchy Nappe with the autochthonous High-Tatric sedimentary cover (Kominy Tylkowe series). It fades out within the ductile marls of Albian age (Zabijak Marlstone Formation — Lefeld *et al*., 1985). Thus this zone, cutting a *ca*. 50 m long section (Kotański, 1959), is exposed along *ca*. 150 m in the field. Its strike is generally parallel to the strike of structures in the Giewont Unit (Jurewicz, 2003), as well as to the course of structural isohypses marking the bottom of the thrust of crystalline rocks belonging to the Giewont Unit (Fig. 1B). Therefore, based on geometrical relations, it seems contemporaneous with the thrusting of the High-Tatric units. It lies at 60° in relation to the thrust surface of the Giewont Unit (Fig. 2A left). After reversing the Tatra block to its position prior to Neogene rotational upheaval (rotation along a horizontal 90/0 axis southwards by 40° — Jurewicz, 2000; comp. Burchart, 1972; Piotrowski, 1978; Janák, 1994), the zone attains a position (Fig. 2A right), which can be interpreted as high-angle R'-type Riedel shears, exhibiting an antithetic sense of displacement — Figure 2B–D (McKinnon and Garrido de la Barra, 1998; Ahlgren, 2001). After rotation, both planes intersect along a 248/18 oriented *b* axis (Fig. 2A right). This orientation is similar to the orientation obtained from stress field reconstruction based on kinematic structure analysis on slickenside surface in the granitoid core (Jurewicz, 2000).

The dislocation zone does not have a uniform and regular internal structure, which results for example from the fact that it runs through different lithological units. In the upper part, within crystalline rocks, the Zadnie Kamienne shear zone recalls mylonitic zones known from the crystalline core of the High Tatra Mts. (Jurewicz and Bagiński, in press). The tectonic zone in this part is 0.5 to 1 m wide and contains a cataclastic gouge (in crystalline rocks) as well as textures indicating brecciation and mylonitization of sedimentary rocks with intense pressure solution processes and mineral veining, recalling structures along the thrust surface at the base of the Giewont Unit (Jurewicz, 2003). In the direct vicinity of the tectonic zone there are small folds, particularly visible in Upper Scythian (Campilian) dark grey dolomites as well as shales and red-grey limestones (beds nos. 18 and 31 in: Kotański, 1959). In its lower part, in the contact zone of the Urgonian limestones and Upper Scythian dolomites, the limestones can be pressed into the dolomites. Urgonian limestones represent isolated clasts in a dolomite mass which acts as matrix (Fig. 2G, H). Dolomites

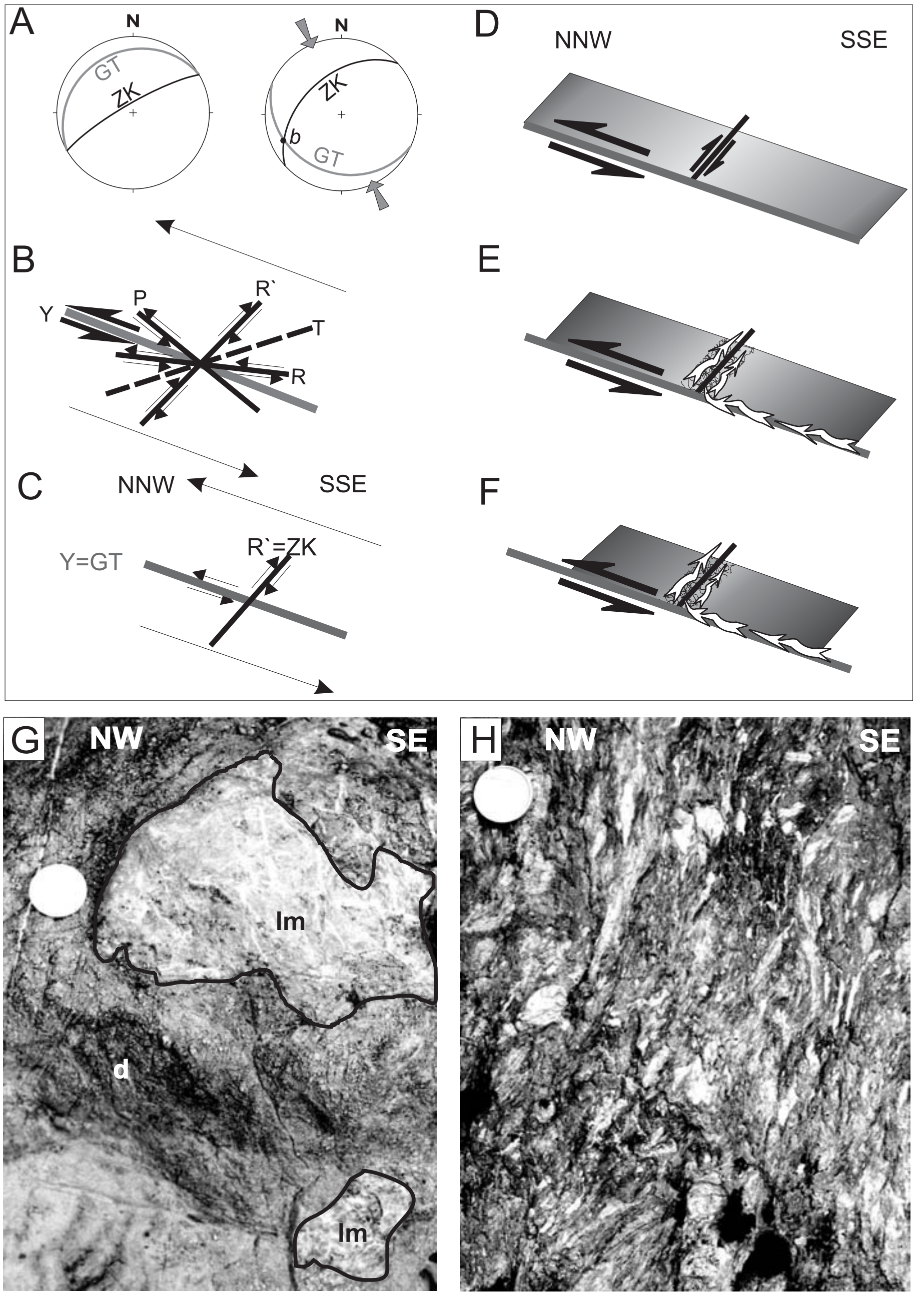

Fig. 2. **A** — orientation of the Zadnie Kamienne shear zone (ZK) in relation to the thrust nappe of the Giewont Unit (GT): left — today, right — prior to the Neogene rotation, *b–b*-axes; **B** — idealized geometry of a Riedel shear zone system (*cf.* Wilcox, 1973; Ahlgren, 2001) Y — principal displacement shear; R, R` — conjugate Riedel shears; R, P — low angle shears, synthetic to the main movement; R` — high angle shear, antithetic to the main movement; **C**, **D** — interpretation of the shear zone of Zadnie Kamienne as R`; **D**–**F** — interpretation of the shear zone of Zadnie Kamienne as a zone of intensive tectonic exaration (“ravenous” shear zone) which provided channel-ways for fluid circulation and mass loss (white arrows). Note that more intense mass loss took place in the hanging wall. Intensive dissolution and mass loss may have compensated for the geometric effect of displacement along R` and relaxes stresses; **G** — fragments (megaclasts) of the Urgonian Osobita Limestone Formation (lm) within the Triassic dolomite (d); there is no evidence of deformation associated with tectonic incorporation of the clasts; scale — a 10 halierov coin; **H** — tectonic melange of limestone and dolomite in the shear zone. Note identical textural ordering of porphyroclasts (stretching lineation and foliation semi-parallel to the wall rocks); scale — a 10 halierov coin

are typically more fractured, which might have favoured the penetration of more ductile limestones along dilatation fissures within the dolomites.

The displacement along the fault zone is rather low in relation to these deformations and does not exceed ~1 m. Stretching lineation and foliation in some places are perpendicular to the shear plane.

STRUCTURES AND TEXTURES

The shear zone generally contains material from the fault walls. The most interesting structures occur in the upper part of the fault zone (Fig. 1C), cutting crystalline rocks of the Giewont Unit, and in the lower part at the contact zone between the Urgonian limestones and Scythian dolomites (Fig. 3A) of the Czerwone Wierchy Nappe (Zdziary Unit). Clasts of limestone of variable size (several — several tens of cm) and shapes (oval, angular, strongly elongated) occur here in a dolomitic mass (Figs. 2G and 3B). The larger clasts of dolomite are usually brittle-fractured (Fig. 4A, B). In some cases the rock seems to comprise alternate elongated clasts of Triassic dolomite and Urgonian limestone (Fig. 2H). The elongation and textural arrangement are distinct macroscopically, where the clasts are several centimetres in size, as well as on microscopic images (Figs. 3C and 4C–F). Some limestones clasts are of mantled porphyroclast character, recognised macroscopically (Fig. 3C). In the well-foliated part of the shear zone with strongly stretched structures and microveins of calcite between them, crenulation folds and crenulation cleavage can be observed (Rajlich, 1993). On Figures 3D and 4C structures of the flattening wedge are developed at the cleavage tips. Surfaces of crenulation cleavage are not regular and are semi-parallel to the shear zone. Distances between the shear surfaces are from several millimetres to 2–3 cm (0.5–3 cm). The pressure solution processes were concen-

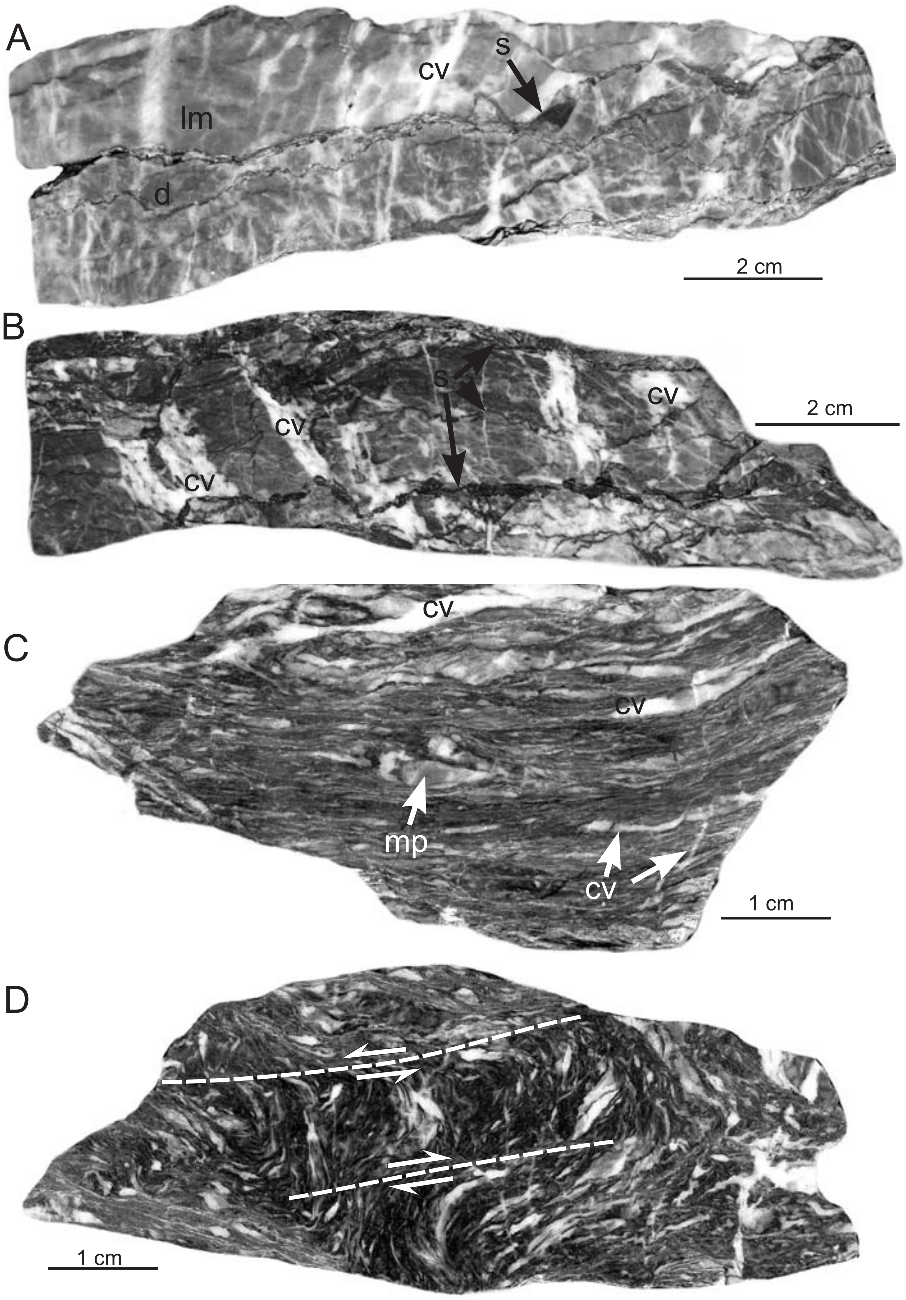

Fig. 3. Different degree of deformation in Urgonian limestones (Osobita Limestone Formation) and Scythian dolomites within the Zadnie Kamienne shear zone; polished surfaces

A — sheet of stylolite (s) along the contact between the Urgonian Osobita Limestone Formation (lm) and Scythian dolomites (d); along the stylolite surface the rock is greenish in colour from chlorite and displays a characteristic detachment; **B** — stylolites (s) between and within clasts of limestone and dolomite; note that the carbonate veins (cv) are in some cases earlier and in other cases later than others; **C** — stretching lineation and foliation within the mylonitized part of the Zadnie Kamienne shear zone; easily visible calcite veins (cv), parallel to mylonitic textures or cutting them, and mantled porphyroclasts (mp — clast of limestone with calcite wings); **D** — deformation of mylonitic textures resembling crenulation cleavage (white dashed lines)

trated along the cleavage surfaces. This cleavage has a fabric of pressure solution cleavage (Nex *et al*., 2003).

Some parts of the Zadnie Kamienne shear zone are composed of tectonic breccias; in turn, others are mylonitic in character — with mylonites defined as foliated and lineated rocks that show evidence of strong and ductile deformation, treated as a strictly structural term that refers only to the fabric of the rock (White *et al*., 1980; Passchier and Trouw, 1998). Dolomite clasts prevail over limestone clasts, which results from the fact that dolomites are less susceptible to dissolution (Kennedy and Logan, 1997; Passchier and Trouw, 1998). The main component of the matrix is a feldspar-clay mineral mass, in which newly formed grains of dolomite, K-feldspar, albite, chlorite, clay and SiO_2 minerals can be identified (see below).

One of the most characteristic deformation processes recognised within the Zadnie Kamienne shear zone includes pressure solution and stylolitic seams linked with this process (Figs. 3A, B and 4D, E). The frequency of pressure solution structures is much higher in the tectonic zones of the Tatra Mts. than in the neighbouring rocks. Stylolitic seams observed under the microscope occur generally along porphyroclast boundaries, and also within them (Fig. 4D). Most of the pressure solution structures of stylolite-character are parallel to the textures and calcite veins. They are evidently younger than the carbonate mineralization (Fig. 3A, B) and only some individual calcite veins cut the stylolite seams (Fig. 4D).

MAIN MINERALS — CONDITIONS OF CRYSTALLIZATION

Components of the mylonitic matrix and residues of the dissolution zones (Fig. 4C–E) were analysed in detail. In mylonitic zones particular attention is drawn to neoformed minerals. In the upper part of the shear zone, where it runs through crystalline rocks, chlorite developed through transformation of biotite and carbonates occurring in the form of veins infilling microshears (Fig. 5A) as well as utilizing twin planes in plagioclases (Fig. 5B), were observed. In the lower part of the dislocation zone, in turn, where Triassic dolomites contact with Urgonian limestones (Kotański, 1959), the mylonitic matrix contains clay and SiO_2 minerals (Figs. 5C, D and 6A, B), K-feldspar (Fig. 5E, F) and albite (Fig. 6C), euhedral grains of dolomite (Fig. 6B, C), as well

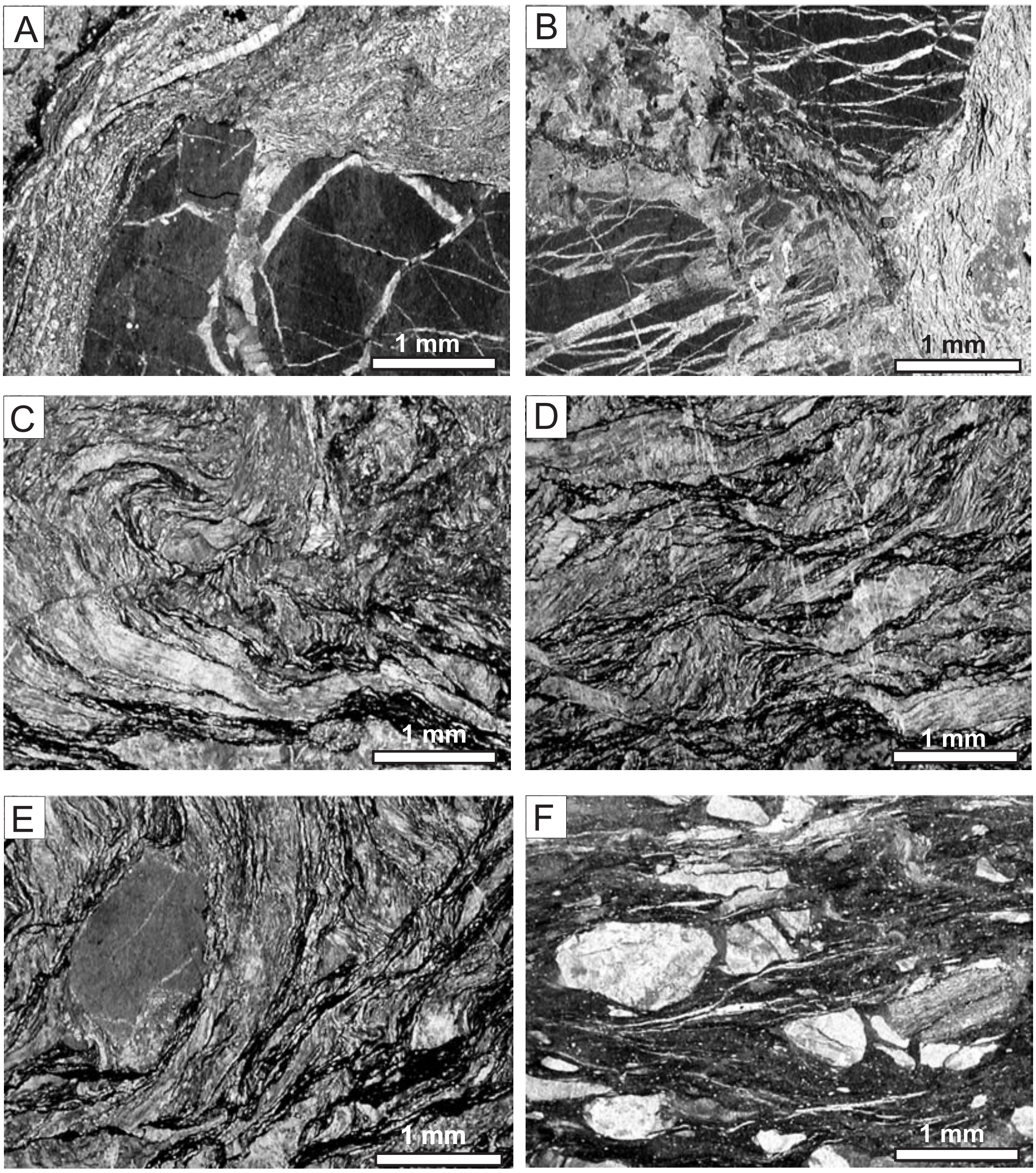

Fig. 4. Different degrees of deformation of rocks from the Zadnie Kamienne shear zone in thin section, non-polarised light

A — brittle-fractured dolomite porphyroclast (calcite-filled gash fractures) and strongly deformed mylonitic matrix with slightly aligned elongated textures; fibrous veins of calcite cutting through the mylonitic matrix and a fragment of the stylolite at the top left are present; **B** — strongly fractured large porphyroclasts of dolomite; carbonate mylonite fills the areas between the clasts; **C**–**E** — non-homogenous deformation of mylonitic textures resembling flow structures; previously parallel-stretched porphyroclasts, later laminated matrix with stylolitization and associated veining; **D** — semi-vertical thin calcite veins cutting earlier mylonitic textures and crossed by stylolites; **E** — large porphyroclast of dolomite within a laminated and deformed mylonitic matrix; **F** — deformed and imbricated porphyroclasts of marls within the mylonitic matrix near the contact of the Albian (Zabijak Marlstone Formation) and Urgonian (Osobita Limestone Formation) rocks in the hanging wall of the Zadnie Kamienne shear zone; pale veins of calcite are visible along microshears

as laths of chlorite (Fig. 6A, B). Within pressure solution zones, developed generally along the mylonitic textures and as stylolites, the residuum comprises feldspar and clay minerals, as well as numerous laths of chlorite. Due to the presence of chlorite these zones have a characteristic green colouring, and the rocks often display partings along these irregular planes.

Carbonates. Besides various sizes of porphyroclasts composed mainly of dolomites and limestone, carbonate veins are frequently present within the Zadnie Kamienne shear zone. Calcite and dolomite occur in form of predeformation veins, mineralising fractures within the porphyroclasts (Fig. 4A, B). Some of the clasts, strongly elongated and folded, are syn-kinematically deformed with carbonate veins — Figure 3C, D. Carbonate veins are most common along the mylonitic structures (Figs. 3C, D and 4A, F), parallel to the shear zone (Teixell *et al*., 2000), locally folded with them (Figs. 3D and 4C) and cut by stylolites and younger calcite veins, which cut the already-formed structures (Figs. 4D and 5G). The relations between dolomite and calcite in mineral veins are well observed on BSE images (Fig. 6A, B). Figure 6A shows calcite fibres

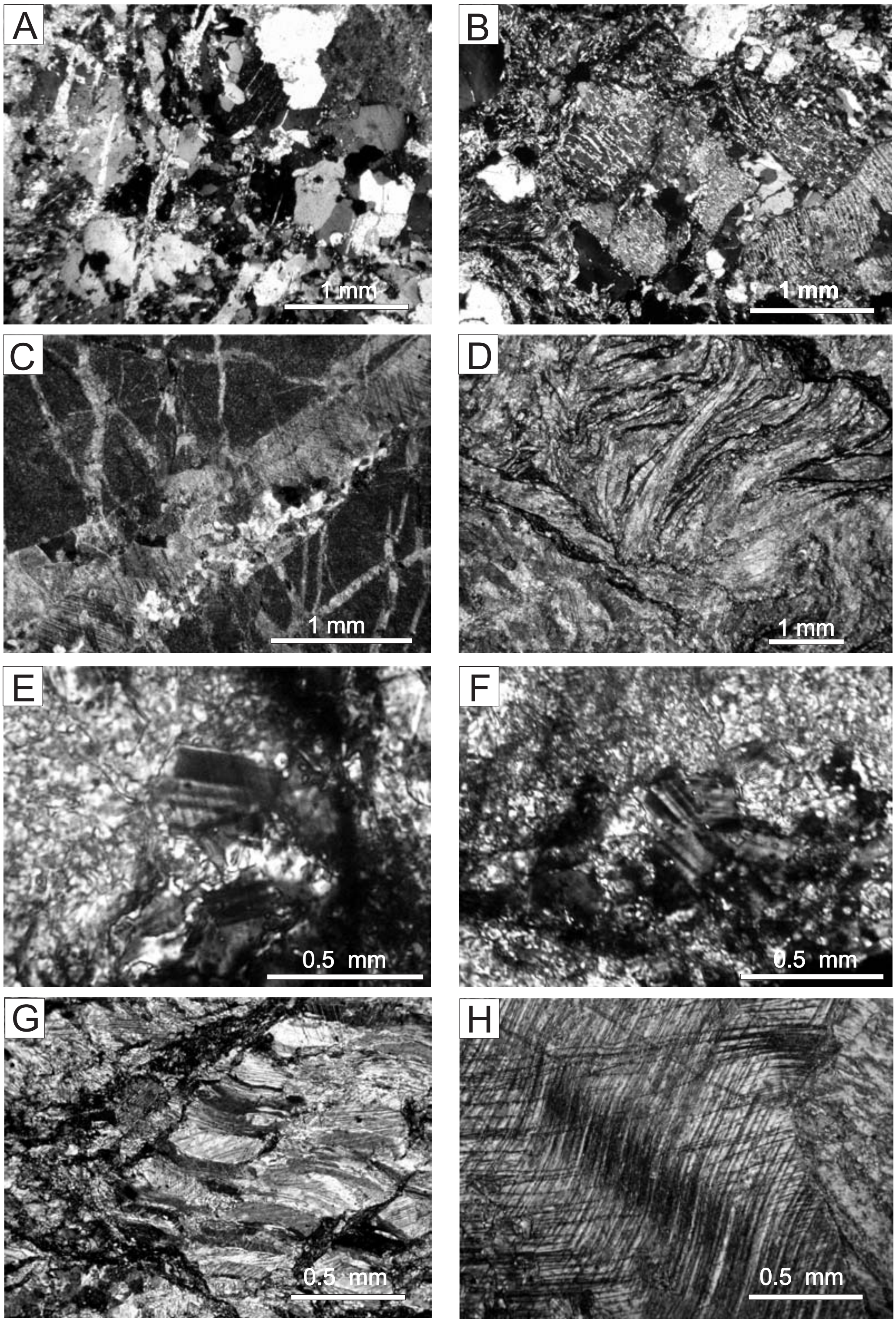

Fig. 5. Thin sections of rocks from the Zadnie Kamienne shear zone in crossed polars

A — calcite veins cutting through mylonitized granitoid rocks related to the Giewont Unit (upper part of the Zadnie Kamienne shear zone); **B** — calcite veins within feldspar grains in mylonitized granitoid rocks of the Giewont Unit; fine-grained calcite crystallized along twin planes in plagioclases and transect them in microshears; **C** — wide calcite vein, younger than the narrow ones, within carbonate clast; fine grains of quartz visible at the bottom side of the vein; **D** — deformations of carbonate rocks; layers are probably represented by stretched clasts of limestone and dolomite; layering is crenulated between shear zones disturbed by pressure solution transfer and the dissolution creep was generated during a younger deformation phase; particular layers and carbonate veins were partly also dissolved by pressure solution; **E**, **F** — euhedral grains of hydrothermal K-feldspar occurring along microshears; **G** — antitaxial vein of carbonate fibres, principally composed of calcite, with poorly visible median line; irregularity of the vein-walls and median line is thought to be due to the activity of pressure solution (stylolitization) and dissolution creep; compare with Figure 6A where the relationship between calcite and dolomite can be seen; **H** — bending of twins in calcite and increase of twin density along the deformation bend and near the grain boundary

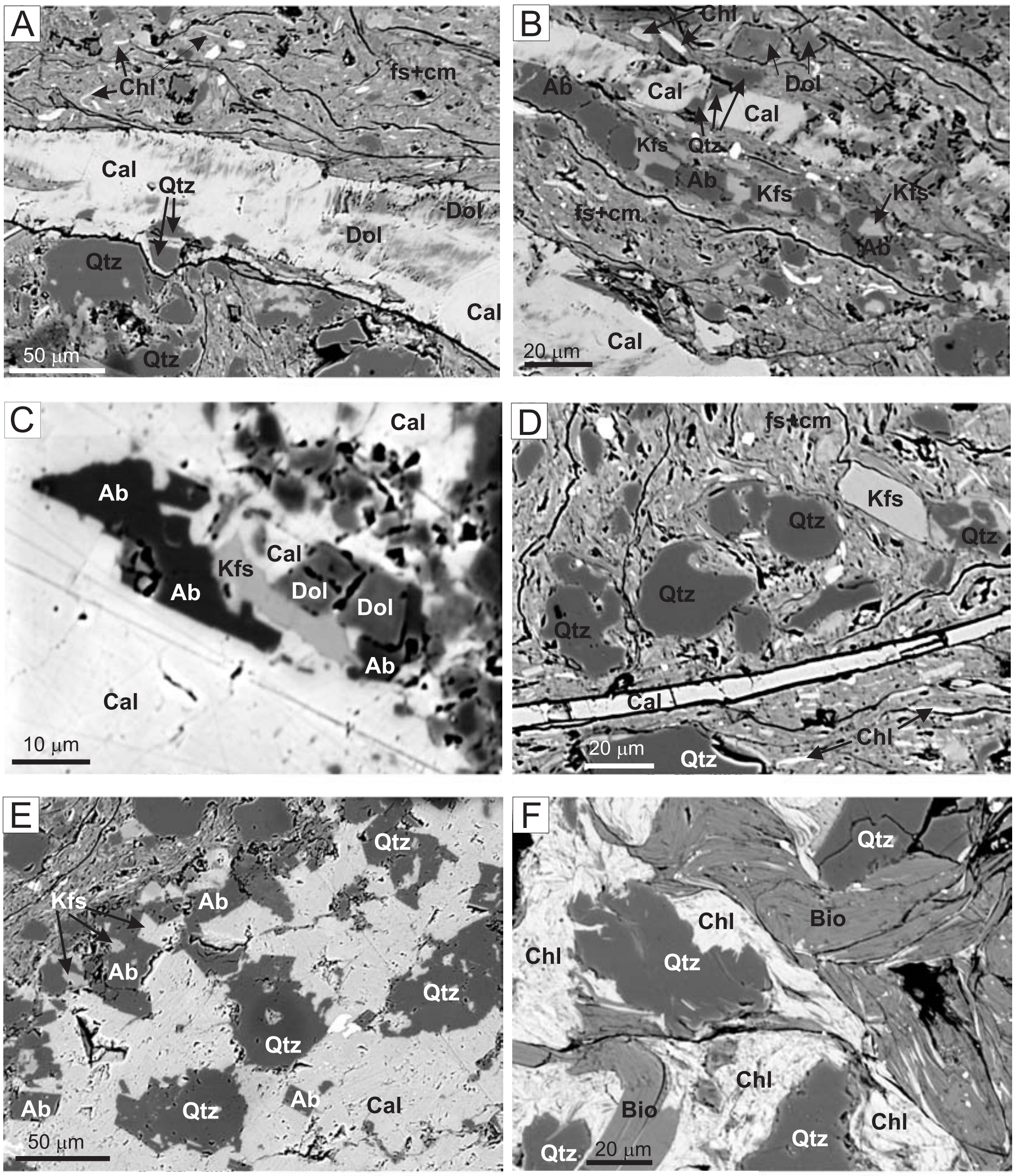

Fig. 6. BSE images (15 keV, 20 nA); **A** — complex carbonate vein within fine-grained mylonitic matrix composed of dolomite, calcite, quartz, K-feldspar, chlorite and clay minerals; note that fibres of dolomite are earlier than calcite; earlier porphyroblast of quartz incorporated into the vein is brittle fractured; at left — relict of median line (fragment of previous mylonitic rocks); **B** — calcite-dolomite and K-feldspar-albite veins in the mylonitic matrix; note numerous euhedral crystals of dolomite within the matrix; **C** — aggregate of albite and K-feldspar and euhedral crystals of dolomite within calcite domain; **D** — thin vein of calcite cutting through the carbonate matrix with quartz and K-feldspar porphyroclasts; **E** — mylonitic matrix at the top right, euhedral and anhedral crystal of albite and K-feldspar and large porphyroclasts of quartz within calcite; **F** — fold deformation of biotite, partly chloritized; mylonitized granitoid rocks related to the Giewont Unit (upper part of the Zadnie Kamienne shear zone); Kfs — potassium feldspar, Ab — albite, Qtz — quartz, Dol — dolomite, Cal — calcite, Chl — chlorite, Bio — biotite, fs+cm — feldspar and clay minerals (symbols of minerals after Kretz, 1983); A–E — part of shear zone within sedimentary rocks, F — part of shear zone within crystalline rocks

normal to the wall rocks growing in dolomite veins (dolomite is earlier). A fragment of the wall-rock as a relict of the median line can be seen on the left of this figure, which points to the primary antitaxial character of this vein. In a later mineralization stage, when calcite appeared instead of dolomite, calcite grew not only on the growth surface but also between the dolomite fibres. In optic microscope images (Fig. 5G), curvatures of fibrous grains, developed probably already during their growth, can be observed. The median line is poorly visible, which is the effect of pressure solution processes and recrystallization that took place along walls of the carbonate vein where stylolites are visible.

Dolomite, well visible on BSE images, besides the porphyroclast and fibrous veins, locally appears within the mylonitic matrix as single euhedral grains (Fig. 6B, C). In single calcite crystals (Fig. 5H) dense twin can be observed, par-

Table 1

Composition of feldspars occurring in the Zadnie Kamienne shear zone

	Na-feldspar						K-feldspar					
	#1	#2	#4	#5	#6	#10	#7	#8	#9	#11	#13	#15
SiO_2	67.57	67.75	68.25	68.33	68.21	67.48	64.90	65.61	63.94	64.76	64.64	64.50
Al_2O_3	19.21	19.21	19.13	19.28	19.23	19.00	17.38	17.60	17.78	17.72	18.03	17.84
CaO	1.27	0.44	0.06	0.08	0.21	0.94	0.41	0.08	0.11	0.03	0.09	0.00
Na_2O	11.75	11.61	11.96	11.89	11.68	11.48	0.14	0.17	0.44	1.67	0.52	0.16
K_2O	0.04	0.10	0.04	0.08	0.05	0.08	16.42	16.34	15.84	14.62	15.91	16.02
FeO	0.00	0.09	0.06	0.02	0.03	0.04	0.00	0.12	0.26	0.09	0.09	0.21
BaO	0.00	0.00	0.00	0.00	0.00	0.00	0.06	0.04	0.55	0.04	0.08	0.07
Totals	99.84	99.20	99.50	99.68	99.41	99.02	99.31	99.96	98.92	98.93	99.36	98.80
Formula on the basis of 8 oxygens												
Si	2.97	3.00	3.00	3.00	3.00	2.99	3.03	3.03	3.01	3.01	3.01	3.02
Al	1.00	0.99	0.99	0.99	1.00	0.99	0.95	0.96	0.99	0.97	0.99	0.98
Ca	0.06	0.02	0.00	0.00	0.01	0.04	0.02	0.00	0.01	0.00	0.00	0.00
Na	1.00	0.99	1.02	1.01	1.00	0.98	0.01	0.02	0.04	0.16	0.05	0.02
K	0.00	0.01	0.00	0.01	0.00	0.00	0.98	0.96	0.95	0.87	0.94	0.96
Totals	5.03	5.01	5.01	5.01	5.01	5.00	4.99	4.97	5.00	5.01	4.99	4.98

ticularly denser near the crystal boundary and in twin deflection zones. After Burkhard (1993), the geometry of e-twins in calcite was applied as a temperature gauge; the bending of twins indicates conditions above 200°C.

Feldspars. In the shear zone of the Zadnie Kamienne close to carbonates, feldspars gather in form of small parallel veins (Fig. 6B). Feldspars occur as single euhedral and subhedral crystals within the microshears in the mylonitic matrix (Figs. 5E, F and 6C). A large proportion of the crystals grew freely, developing their own, mostly rhombohedral, habit. The crystals are transparent and devoid of inclusions. Their composition, determined on the basis of microprobe analysis (Table 1), indicates a prevalence of potassium-enriched feldspars over sodium-enriched ones. The recalculated formula places them close to pure albite and adularia (Table 1). Despite the domination of the orthoclase molecule in the adularia and of the albite molecule in the albite, the analysed feldspars represent the ternary composition Ab-An-Or. The anorthite particle accompanies, in minor amounts, some of the alkali feldspars. Albites and adularia recovered from the Zadnie Kamienne shear zone have a poorly marked domain structure. Potassium feldspars reveal slight undulose extinction. The growth morphology of sodium feldspars recalls poorly developed chess-board twinning. The feldspars occur within a matrix composed of carbonates, feldspars and clay minerals, SiO_2 minerals and chlorites (Fig. 6B, D, E).

The habit of the feldspars and their composition argue for a hydrothermal origin. The rhombohedral shape of the crystals is common among hydrothermal adularia. Transparency, referred to as "water clear" is a typical feature of hydrothermal feldspars. By contrast detrital feldspars are dusty. The composition of the investigated feldspars is also characteristic of low-temperature formation processes. Crystallization of feldspars under hydrothermal conditions is highly correlated with sodium, potassium and proton activity in the solution (Giggenbach, 1984; Słaby *et al*., 1993), although other factors may also control this process. The process usually takes place under non-equilibrium conditions, often far from equilibrium. The degree of deviation from the equilibrium state reflects the pattern of the feldspar growth morphology and the order-disorder of their structure (Słaby, 1990, 1992, 2000). The habit of the feldspar displays mostly a domain, patchy, tiled, or

Table 2

Estimation of feldspars crystallization temperature

	Ab	Or	An	Average
"A"	Nekvasil and Burnham model (1987)			
Temperature [°C]	421.95	312.85	421.95	385.58
Plagioclase (composition)	0.957	0.004	0.04	–
K-feldspar (composition)	0.092	0.893	0.007	–
"B"	Fuhrmann and Lindsley model (1988)			
Temperature [°C]	348.37	348.37	348.37	348.37
Plagioclase (composition)	0.99	0.004	0.052	–
K-feldspar (composition)	0.085	0.91	0.003	–

Ab — albite, Or — orthoclase, An — anorthite; other explanations see text

Table 3

Composition of chlorites occurring within mylonites of the Zadnie Kamienne shear zone (sample 1 — from crystalline rocks, another — from sedimentary rocks)

Chlorites													
	high-ferruginous				low-ferruginous		formula on the basis of 14 oxygens						
	#1	#4	#8	#10	#21	#22		#1	#4	#8	#10	#21	#22
SiO_2	25.32	25.88	26.45	28.14	33.53	33.98	Si	2.80	2.83	2.86	2.80	3.29	3.32
TiO_2	0.15	0.06	0.03	0.09	0.03	0.00	Ti	0.01	0.00	0.00	0.00	0.00	0.00
Al_2O_3	20.80	21.61	20.25	21.63	15.52	15.85	Al^{IV}	1.20	1.17	1.14	1.20	0.71	0.68
MgO	7.57	7.58	8.39	23.90	27.32	26.85	Al^{VI}	1.51	1.61	1.53	1.34	1.09	1.14
CaO	0.05	0.05	0.12	0.16	0.40	0.37	Mg	1.25	1.23	1.37	3.55	3.99	3.90
MnO	0.10	0.07	0.05	0.04	0.02	0.01	Ca	0.01	0.01	0.01	0.02	0.04	0.04
FeO	32.96	31.44	31.50	11.87	8.34	8.37	Mn	0.01	0.01	0.00	0.00	0.00	0.00
Na_2O	0.02	0.02	0.00	0.02	0.01	0.04	Fe	3.05	2.88	2.88	0.99	0.69	0.68
K_2O	0.14	0.24	0.08	0.08	0.02	0.08	Na	0.01	0.00	0.00	0.00	0.00	0.01
H_2O	10.84	10.97	10.96	12.03	12.23	12.29	K	0.02	0.04	0.01	0.01	0.00	0.01
Totals	97.82	97.92	97.83	97.96	97.42	97.84	Totals	9.87	9.78	9.80	9.90	9.81	9.78

twinned pattern. This in turn reflects their optic heterogeneity. The more dynamic is the growth of feldspars, the better the heterogeneity is developed (Słaby, 2000). It seems therefore that the domain pattern of the investigated feldspars, both Na- and K-rich, took place in conditions close to equilibrium. Kinetically — driven growth should be excluded. The growth morphology and composition exclude also a detrital character for the analysed feldspars.

Similarly, the presence of the anorthite and albite molecules in the adularia, and anorthite and orthoclase in the albite, indicate conditions close to equilibrium. This might point to proper distribution of potassium, sodium and calcium between Na- and K-rich feldspars during the crystallization process. The compositions of some of the pairs are located on the low-temperature part of the feldspar solvus. These might be arguments in favour of using two-feldspar models for temperature estimation. The attempt to use the models has to be, however, treated with great caution. Crystallization of minerals in hydrothermal conditions is controlled on the one hand by temperature and on the other hand by the concentrations of particular species within the solutions. The relation of the two factors is impossible to determine in the case of fossil examples. Two-feldspar crystallization models were used in calculations by Nekvasil and Burnham (1987) and by Fuhrmann and Lindsley (1988). The models are constructed for feldspars growing under magmatic conditions, however, post-magmatic processes, such as coarsening at low temperature, could be evaluated using the models. Two of the analysed hydrothermal feldspar pairs gave positive results. For one of the analysed pairs "A" (Table 2) the positive result was obtained with the Nekvasil and Burnhamm thermometer, while the second "B" was obtained with the Fuhrmann and Lindslay thermometer. The crucial objection lies in the fact that both models cannot be applied for the two pairs. The temperatures obtained are similar, although the character of crystallization is different. Pair "A" indicates 385°C as the crystallization temperature. It took place in conditions far from equilibrium $|dT| = -218.19$. Pair "B" crystallized in equilibrium with the environment $|dT| = 0.00$ at a temperature of 348°C. In a hydrothermal system, which is an open system, both cases probably took place in close vicinity to one another. On the other hand, it is possible that both results are far from reality, if the influence of temperature on crystallization of both feldspars in pairs was minimal.

Chlorite. Single laths of chlorite occur very often in the mylonitic matrix within the lower part of Zadnie Kamienne shear zone (Fig. 6A, B, D). The composition of these crystals varies significantly. Within the crystals two compositionally different populations, low-ferruginous and high-ferruginous (Table 3), can be distinguished. In the upper part, where the shear zone cuts the granitoid rocks of the crystalline core of the Giewont Unit, the high-ferruginous type of chlorite has been found (thin sheets within folded crystals of biotite — Figure 6F). Small chlorite lenses intercalate with the biotite plates. Their composition is usually non-stoichiometric and only one analysis was included in the table data (Table 3, no. 1). Biotite, accompanied by chlorite laths, is strongly folded (Fig. 6F). Stesky (1978) suggested that biotite has ductile behaviour at temperatures above 250°C.

Chlorite appears in a paragenesis with hydrothermal feldspars in the lower part of the Zadnie Kamienne shear zone, within the mylonitized sedimentary rocks. The reconstructed thermal conditions by means of feldspar pairs could be corroborated by other methods. Chlorite paragenesis with feldspars may provide additional information. Based on tetrahedral and octahedral site occupancy (Cathelineau, 1988), the crystallization temperature of chlorite has been estimated. The data obtained indicate that the chlorites seemed to crystallize in two thermally different events: $T_1 \approx 292$–357°C and $T_2 \approx 155$–167°C. The higher temperature event correlates well with the temperature estimated using feldspar models. Chlorite from the upper part of the shear zone (Table 3, no. 1), being the decay product of biotite, has been used for thermal evaluation, and indicated a temperature comparable to episode T_1 (~ 325°C).

DISCUSSION

The Zadnie Kamienne shear zone is a high-angle Riedel type shear zone (R'), which may have developed synchronously with the nappe-thrusting of the High-Tatric Nappes. Deformations occurring along this zone including mylonitization, stretching lineation, foliation, pressure solution accompanied by precipitation and vein-forming, are very similar to structures occurring along the thrust-fault at the base of the Giewont Unit (Jurewicz, 2003) and along other thrust surfaces in the Tatra Mts. (Kotański, 1956, 1959; Bac-Moszaszwili *et al*., 1981; Jaroszewski, 1982). Shear zones like this provide channel-ways for fluid circulation and play an important role in the mass loss (Vernon, 1998). The mass reduction caused only by chemical compaction of the condensed Middle Jurassic deposits in the High-Tatric series was assessed by Łuczyński (2001) at about 20–70%. In the shear zone, estimating the mass loss value based on the residuum is difficult due to the high lithological variability of the Triassic strata and the possible removal of a large volume of rocks in suspension beyond the tectonic zone (see Gratier *et al*., 1999; Renard *et al*., 2000; Jurewicz, 2003).

The amount of displacement along this zone is very low and does not correlate with the strength and ductile character of the deformations and therefore another explanation of this phenomenon is plausible. The lack of unequivocal indicators of shearing and the minor geometrical effect of the displacement could partly reflect the change of direction of movement and its oscillatory character. This is suggested by folding of mylonitic textures both in the crystalline and sedimentary rock sections of the tectonic zone, as well as by local rotation of elongation textures to positions almost perpendicular to the wall rocks. Their formation might be linked with a multiple tectonic reactivation and repeated periods of brecciation and fluidization (Newman and Mitra, 1994; Branquet *et al*., 1999). Pulsation movements taking place along the shear zone could have been initiated in the same way as along the thrust surface by pulsatory changes of pore pressure (Küster and Stöckhert, 1999; Branquet *et al*., 1999), and accompanying stages of dissolution along the stylolite, precipitation and vein-forming (Petit *et al*., 1999; Karcz and Scholz, 2003). Processes such as these linked with hydrotectonic phenomena were described by Bac-Moszaszwili *et al*. (1981), Jaroszewski (1982) and Jurewicz (2003) from the Polish Tatra Mts. and Milovský *et al*. (2003) from the Silicicum cover nappe system. These processes responsible for shape and volume transformation accompanied by mass loss have the character of large-scale volume-diffusion creep (Davis and Reynolds, 1996). Dissolution along stylolites can be thought as a mechanism of stress relaxation within and around the fault (Renard *et al*., 2000) and may compensate the geometrical effect of displacement (Fig. 2D–F). We propose to call a shear zone, within which mass reduction plays a more important role in the relaxation of stress than the displacement, a "ravenous" shear zone.

Analysis of feldspar crystallization conditions indicated that the Zadnie Kamienne shear zone was a migration pathway for hydrothermal solutions, which influenced the deformation conditions and the character of structures occurring within it. The growth morphology of the feldspars found in the shear zone of Zadnie Kamienne indicates unequivocally their crystallization under hydrothermal conditions. Hydrothermal crystals of feldspar are concentrated particularly along the microshears. The presence of authigenic crystals of potassium feldspar was noted by Plašienka and Soták (1996) in the matrix of rauwacke. Milovský *et al*. (2003) described it in basal cataclasites of the Muráň Nappe and Jurewicz (2003) in mylonites from the base of thrust-nappes of the Giewont Unit (High-Tatric Nappe).

The composition of the neo-formed minerals occurring within this zone has been used for calculating the thermal conditions of these processes. Simultaneous growth of albite and adularia indicates a temperature of about 350°C. Chlorites accompanying them occur in two thermal episodes, where the first one (T_1) points to a similar temperature (292–357°C). The temperature of feldspar — T_1-chlorite crystallization varies in a quite narrow range and is slightly higher in relation to that determined on the basis of petrotectonic analysis.

For structures occurring along the thrust-fault at the base of the Giewont Unit the estimated temperature is *ca*. 300°C (Jurewicz 2003). It is also much higher than temperatures obtained on the basis of fluid inclusion analysis in quartz formed on surfaces of slickensides in the crystalline core of the High Tatra Mts. recorded by fluid inclusion temperatures of 212–254°C at pressures of 1.45–1.73 kbar (Jurewicz and Kozłowski, 2003), indicating an overburden of 6–7 km and a geothermal gradient of *ca*. 30°C (Jurewicz and Bagiński, in press). Deformation in the High-Tatric Nappes lying on the para-autochthonous sedimentary cover must have taken place under a smaller, *ca.* 1–2 km thick overburden and at lower temperatures. The deformation was accompanied by the activity of hydrothermal solutions. The solutions operating within the zone led to the formation of feldspar and chlorite from group T_1 under similar thermal conditions. Likewise, the feldspar growth morphology strongly corroborated the presence of hydrothermal processes in the shear zone. The observed changes within such a minor dislocation along the shear zone cannot be explained by pure dynamometamorphism.

Much higher temperatures after fluid inclusion investigations — between 213 and 471°C — were obtained by Milovský *et al*. (2003) from basal cataclasites of the Muráň Nappe. Such high temperatures are explained as a reflection of locally supralithostatic overpressures induced by frictional heating beneath the moving nappe. Probably similar processes developing at the base of the High Tatric Nappes (Jurewicz, 2003) were the source of high-temperature fluids which flowed along the shear zone (and also Riedel shears) according to the local hydraulic gradient (Sibson, 1996).

CONCLUSIONS

1. The Zadnie Kamienne shear zone is a high-angle Riedel type shear zone (R') exhibiting an antithetic sense of displacement. It may have developed synchronously with the nappe-thrusting of the High-Tatric Nappes.

2. This zone was the pathway of migration for hydrothermal solutions, which influenced the deformation conditions and the character of structures occurring within it.

3. Tentative application of feldspar and chlorite geothermometers allowed quantifying the hydrothermal solution temperature at up to ~ 350°C.

4. The Zadnie Kamienne shear zone can be interpreted as a zone of intense dissolution creep and mass loss with very small dislocation, causing stress relaxation without displacement, and may be called a "ravenous" shear zone.

Acknowledgements. This research was supported by an individual BW grant no. 1567/2. The authors would like to express their gratitude to Dr. R. Milovský and an anonymous review for critical reading of the manuscript and for fruitful discussion. We are grateful to Dr. B. Bagiński for aid with chlorite investigations, L. Jeżak M.Sc. for help with microprobe analysis and Dr. A. Żylińska for linguistic advice. Thanks are also due to the Direction of the Tatra National Park for permission to conduct fieldwork.

REFERENCES

AHLGREN S. G. (2001) — The nucleation and evolution of Riedel shear zones as deformation bands in porous sandstone. J. Struct. Geol., **23** (8): 1203–1214.

ANDRUSOV D. (1965) — Aperçu générale sur la géologie des Carpathes occidentales. Bull. Soc. Géol. France, **7**: 1029–1062.

BAC-MOSZASZWILI M., BURCHART J., GŁAZEK J., IWANOW A., JAROSZEWSKI W., KOTAŃSKI Z., LEFELD J., MASTELLA L., OZIMKOWSKI W., RONIEWICZ P., SKUPIŃSKI A. and WESTFALEWICZ-MOGILSKA E. (1979) — Mapa geologiczna Tatr Polskich 1:30 000. Wyd. Geol. PAN, Pol. Tow. Geol.

BAC-MOSZASZWILI M., GAMKERLIDZE I. P., JAROSZEWSKI W., SCHROEDER E., STOJANOV S. and TZANKOV T. V. (1981) — Thrust zone of the Križna Nappe at Stoły in Tatra Mts (Poland). Stud. Geol. Pol., **68**: 61–73.

BAC-MOSZASZWILI M., JAROSZEWSKI W. and PASSENDORFER E. (1984) — On the tectonics of Czerwone Wierchy and Giewont area in the Tatra Mts., Poland (in Polish with English summary). Ann. Soc. Geol. Pol., **52** (1–4): 67–88.

BRANQUET Y., CHEILLETZ A., GILLIANI G., LAUMONIER B. and BLANCO O. (1999) — Fluidized hydrothermal breccia in dilatant faults during thrusting: the Colombian emerald deposits. In: Fractures, Fluid Flow and Mineralization (eds. K. J. W. McCaffrey, L. Lonergan and J. J. Wilkinson). Geol. Soc. Spec. Publ., **155**: 182–195.

BURCHART J. (1972) — Fission-track age determination of accessory apatite from the Tatra Mts, Poland. Earth Plane. Sc. Lett., **15**: 418–422.

BURKHARD M. (1993) — Calcite-twins, their geometry, appearance and significance as stress-strain markers and indicators of tectonic regime: a review. J. Structur. Geol., **15**: 351–368.

CATHELINEAU M. (1988) — Cation site occupancy in chlorites and illites as a function of temperature. Clay Minerals, **23**: 471–485.

DAVIS G. H. and REYNOLDS S. J. (1996) — Structural Geology. John Wiley and Sons, Inc.

FUHRMANN M. L. and LINDSLEY D. L. (1988) — Ternary-feldspar modelling and thermometry. Am. Miner., **73**: 201–215.

GIGGENBACH W. F. (1984) — Mass transfer in hydrothermal alteration systems. A conceptual approach. Geochim. Cosmochim. Acta, **48**: 2693–2711.

GRATIER J. P., RENARD F. and LABAUME P. (1999) — How pressure solution creep and fracturing process interact in the upper crust to make it behave in both a viscous and brittle manner. J. Structur. Geol., **21** (8–9): 1189–1197.

GUZIK K. (1959) — Mapa geologiczna Tatr polskich ark. Kominy Tylkowe, 1:10 000. Inst. Geol.

JANÁK M. (1994) — Variscan uplift of the crystalline basement, Tatra Mts, Central West Carpathians: evidence from $^{40}Ar/^{39}Ar$ laser probe dating of biotite and P-T-t paths. Geol. Carpath., **45** (5): 239–300.

JAROSZEWSKI W. (1982) — Hydrotectonic phenomena at the base of the Križna Nappe, Tatra Mts. In: Alpine Structural Elements: Carpathian-Balkan-Caucasus-Pamir Orogene Zone, Veda, Bratislava (ed. M. Mahel'): 137–148.

JUREWICZ E. (2000) — Tentative reconstructions of the stress axes from the thrust-folding stage in the Tatra Mts. on the basis of slickensides in the granitoid core, southern Poland (in Polish with English summary). Prz. Geol., **48** (3): 239–246.

JUREWICZ E. and KOZŁOWSKI A. (2003) — Formation conditions of quartz mineralization in the mylonitic zones and on the slickenside fault planes in the High Tatra granitoids. Archiw. Miner., **54**: 65–75.

JUREWICZ E. (2003) — Multistage evolution of the shear zone at the base of the Giewont Unit, Polish Tatra Mts. Geol. Carpat., **54** (5): 337–351.

JUREWICZ E. and BAGIŃSKI B. (2005) — Deformation phases in the selected shear zones within the Tatra Mts granitoid core. Geol. Carpat. (in press).

KARCZ Z. and SCHOLZ C. H. (2003) — The fractal geometry of some stylolites from the Calcare Massiccio Formation, Italy. J. Structur. Geol., **25** (8): 1301–1316.

KENNEDY L. A. and LOGAN J. M. (1997) — The role of veining and dissolution in the evolution of fine-grained mylonites: the McConnell thrust, Alberta. J. Structur. Geol., **19** (6): 785–797.

KOTAŃSKI Z. (1956) — High-Tatric Campillian in the Tatra Mts. (in Polish with English summary). Acta Geol. Pol., **6** (1): 65–73.

KOTAŃSKI Z. (1959) — Stratigraphical sections of the high-Tatric Series in the Polish Tatra Mts. (in Polish with English summary). Biul. Inst. Geol., **139**.

KOTAŃSKI Z. (1965) — La structure géologique de la chaine subtatrique entre la vallée de Mała Łąka et la vallée Kościeliska dans les Tatras Occidentales (in Polish with French summary). Acta Geol. Pol., **15** (3): 257–320.

KRAJEWSKI K. (1980) — Z badań sedymentologicznych utworów kredy wierchowej w Dolinie Kościeliskiej. Prz. Geol., **28** (11): 636–637.

KRETZ R. (1983) — Symbols for rock-forming minerals. Am. Miner., **68**: 277–279.

KÜSTER M. and STÖCKHERT B. (1999) — High differential stress and sublithostatic pore fluid pressure in the ductile regime — microstructural evidence for short-term post-seismic creep in the Sesia Zone, Western Alps. Tectonophysics, **303** (1–4): 263–277.

LEFELD J., GAŹDZICKI A., IWANOW A. and KRAJEWSKI K. (1985) — Jurassic and Cretaceous lithostratigraphic units of the Tatra Mts. Stud. Geol. Pol., **84**.

ŁUCZYŃSKI P. (2001) — Pressure-solution and compaction of condensed Middle Jurassic deposits, High Tatric series, Tatra Mts. Geol. Carpat., **52** (2): 91–102.

MCKINNON S. D. and GARRIDO DE LA BARRA I. (1998) — Fracture initiation, growth and effect on stress field: a numerical investigation. J. Structur. Geol., **20** (12): 1673–1689.

MILOVSKÝ R., HURAI V., PLAŠIENKA D. and BIROŇ A. (2003) — Hydrotectonic regime at soles of overthrust sheets: textural and fluid inclusion evidence from basal cataclasites of the Muráň nappe (Western Carpathians, Slovakia). Geodinam. Acta, **16**: 1–20.

NEKVASIL H. and BURNHAM C. W. (1987) — The calculated individual effects of pressure and water content on phase equilibria in the granite system. In: "Magmatic Processes: Physicochemical Principles (ed. B. O. Mysen). University Park, Pa.: Geochemical Society".

NEWMAN J. and MITRA G. (1994) — Fluid influenced deformation and recrystallization of dolomite at low temperatures along a natural fault zone, Mountain City window, Tennessee. Geol. Soc. Am. Bull., **106** (10): 1267–1279.

NEX P. A., KINNAIRD J. A. and IXER R. A. (2003) — Localized ductile thrusting north of the Variscan Front, Ross Island, southwest Ireland. Geol. J., **38** (1): 15–29.

PASSCHIER C. W. and TROUW R. A. J. (1998) — Microtectonics. Springer-Verlag.

PETIT J. P., WIBBERLEY C. A. J. and RUIZ G. (1999) — "Crack-seal", slip: a new fault valve mechanism? J. Structur. Geol., **21** (8–9): 1199–1207.

PIOTROWSKI J. (1978) — Mesostructural analysis of the main tectonic units of the Tatra Mts. along the Kościeliska Valley. Stud. Geol. Pol., **55**.

PLAŠIENKA D. and SOTÁK J. (1996) — Rauwackized carbonate tectonic breccias in the West Carpathian nappe edifice: introductory remarks and preliminary results. Slovak Geol. Magaz., **3**–**4**: 287–291.

RENARD F., GRATIER J. P. and JAMTVEIT B. (2000) — Kinetics of crack-sealing, intergranular pressure solution, and compaction around active faults. J. Structur. Geol., **22** (10): 1395–1407.

RAJLICH P. (1993) — Riedel shear: a mechanism for crenulation cleavage. Earth Sc. Rev., **34** (3): 167–195.

SIBSON R. H. (1996) — Structural permeability of fluid-driven fault-fracture meshes. J. Structur. Geol., **18** (8): 1031–1042.

SŁABY E. (1990) — Adularia from Miękinia (in Polish with English summary). Archiw. Miner., **46** (1–2): 55–69.

SŁABY E. (1992) — Changes in the structural state of secondary albite during progressive albitization. Neues Jahrb. Miner., Monatsh., **H7**: 321–335.

SŁABY E. (2000) — Sodium and potassium feldspars — products of late magmatic alteration. Pr. Spec. Pol. Tow. Miner., **17**: 35–38.

SŁABY E., KOZŁOWSKI A., LENSCH G. and MIHM A. (1993) — Origin of albite-adularia paragenesis — an example of alkali metasomatism through magmatic-meteoric fluid mixing. Miner. Pol., **24** (1–2): 3–19.

STESKY R. M. (1978) — Mechanisms of high temperature frictional sliding in Westerly granite. Canad. J. Earth Sc., **15**: 361–375.

TEIXELL A., DURNEY D. W. and ARBOLEYA M. L. (2000) — Stress and fluid on décollement within competent limestone. J. Structur. Geol., **22** (3): 349–371.

VERNON R. H. (1998) — Chemical and volume changes during deformation and prograde metamorphism of sediments. In: What Drives Metamorphism and Metamorphic Reactions? (eds. P. J. Treloar and P. J. O'Brien). Geol. Soc., London. Spec. Public., **138**: 215–246.

WHITE S. H., BURROWS S. E., CARRERAS J., SHAW N. D. and HUMPHREYS F. J. (1980) — On mylonites in ductile shear zones. J. Structur. Geol., **2**: 175–187.

WILCOX R. E., HARDING T. P. and SELLY D. R. (1973) — Basic wrench tectonics. Am. Ass. Petrol. Geol. Bull., **57**: 74–96.